JPn Neuroscience
The Journal of Physiology

J Physiol 590.22 (2012) pp 5563–5569

TOPICAL REVIEW

Synaptic integration in dendrites: exceptional need for speed

Nace L. Golding[1] and Donata Oertel[2]

[1] *Section of Neurobiology and Center for Learning and Memory, University of Texas at Austin, Austin, TX, USA*
[2] *Department of Neuroscience, University of Wisconsin, School of Medicine and Public Health, Madison, WI, USA*

Abstract Some neurons in the mammalian auditory system are able to detect and report the coincident firing of inputs with remarkable temporal precision. A strong, low-voltage-activated potassium conductance (g_{KL}) at the cell body and dendrites gives these neurons sensitivity to the rate of depolarization by EPSPs, allowing neurons to assess the coincidence of the rising slopes of unitary EPSPs. Two groups of neurons in the brain stem, octopus cells in the posteroventral cochlear nucleus and principal cells of the medial superior olive (MSO), extract acoustic information by assessing coincident firing of their inputs over a submillisecond timescale and convey that information at rates of up to 1000 spikes s^{-1}. Octopus cells detect the coincident activation of groups of auditory nerve fibres by broadband transient sounds, compensating for the travelling wave delay by dendritic filtering, while MSO neurons detect coincident activation of similarly tuned neurons from each of the two ears through separate dendritic tufts. Each makes use of filtering that is introduced by the spatial distribution of inputs on dendrites.

(Received 8 June 2012; accepted after revision 22 August 2012; first published online 28 August 2012)
Corresponding author D. Oertel: Department of Neuroscience, School of Medicine and Public Health, University of Wisconsin, 1300 University Ave, Madison, WI 53706, USA. Email: doertel@wisc.edu

Introduction

Neurons in the brain stem that receive and convey acoustic information in the timing of firing serve as coincidence detectors that work at a time scale of tens or hundreds of microseconds and can fire at high rates, up to 1000 spikes s^{-1}. The speed of these neurons is made possible by the morphology, synaptic properties and by the presence of voltage-sensitive conductances that produce low input resistances and short time constants. The high temporal resolution of these neurons makes them sensitive to the morphological and biophysical properties of dendrites and to the spatial distribution of synaptic inputs. Octopus cells make use of dendritic filtering to compensate for cochlear travelling wave delays in detecting broadband transient sounds. Principal cells of the medial superior olivary nucleus use dendrites to

Nace L. Golding (left) completed his graduate work in Donata Oertel's lab, where among other projects, he first raised the question of how octopus cells could detect synchrony in inputs that are by nature asynchronous. As a postdoc with Nelson Spruston at Northwestern University he examined dendritic excitability and synaptic plasticity in the hippocampus. He now combines his interests in dendritic processing and auditory circuits as an associate professor at UT-Austin, where he has been since 2002. **Donata Oertel** (right) began her career with work on firefly light organs, electrical excitability in paramecia and vision in barnacles at UC Santa Barbara, University of Wisconsin and Harvard Medical School, respectively. Her interests were drawn to the auditory system by Bill Rhode, Jerzy Rose, Joe Hind and Dan Geisler when she returned to rejoin her husband in Madison. She has used brain slices to understand how acoustic information is processed by the cochlear nuclei since 1981.

DOI: 10.1113/jphysiol.2012.229328

enhance detection of coincidence of inputs from the two ears.

Octopus cells sense sweeps of excitation in populations of auditory nerve fibres

Broadband transient sounds, such as the snapping of branches and the onsets of many consonants in human speech, represent a sudden increase in acoustic energy over wide frequency regions and are common features of natural sounds. In the cochlea broadband transients evoke a travelling wave that activates fibres tuned to high frequencies before it activates those tuned to low frequencies, producing a sweep of firing of auditory nerve fibres from those tuned to high frequencies to those tuned to low frequencies. Total travelling wave delays are about 8 ms in mammals that hear low frequencies (including cats, dogs and humans) and 1.6 ms in small mammals that hear only high frequencies (mice) (Ruggero, 1992; McGinley *et al.* 2012). The inputs to any one octopus cell vary over a fraction (∼1/3) of the total travelling wave delay. Octopus cells respond to clicks, to the onsets of tones and to loud low-frequency tones with sharply timed action potentials at rates up to 800 s^{-1} (Godfrey *et al.* 1975; Rhode *et al.* 1983; Rhode & Smith, 1986; Oertel *et al.* 2000; Smith *et al.* 2005). The axons of octopus cells innervate the contralateral ventral nucleus of the lateral lemniscus (Adams, 1997; Smith *et al.* 2005) and, perhaps, the superior paraolivary nucleus (Schofield, 1995).

MSO neurons assess coincidence in the timing of signals from each of the two ears

Interaural time differences (ITDs) are cues about the angle from which sounds arise with respect to the front. In mammals that hear low-frequency sounds (<2 kHz), principal cells of the MSO modulate their firing rates over a narrow range of ITDs so that information contained in their firing can be used for localizing sounds. Jeffress (1948) proposed that sensitivity to different ITDs could be conferred by differences in the length of excitatory axons innervating MSO neurons from each ear (forming so-called 'delay lines'). While there is evidence for such a wiring-based mechanism in birds (Carr & Konishi 1990; Burger *et al.* 2011), the situation in mammals is less settled (Joris & Yin, 2007). The natural range of ITDs in mammals depends on the size of the head, ranging from 120 μs in gerbils (rodents with good low-frequency hearing) to >700 μs in humans. Gerbils and human subjects resolve ITDs as low as 40 and 10 μs, respectively (Mills, 1958; Maier & Klump, 2006). MSO neurons convey information mainly to the ipsilateral dorsal nucleus of the lateral lemniscus (Henkel, 1997) and inferior colliculus (Henkel & Spangler, 1983; Nordeen *et al.* 1983).

Arrangement of synapses on dendrites shapes synaptic integration and function

Octopus cells spread their dendrites across the tonotopically organized bundle of auditory nerve fibres where fibres pass from the ventral to the dorsal cochlear nucleus (Fig. 1*A*). Dendrites in mice are thick, primary branches about 4 μm in diameter, and between 100 and 200 μm long. In mice about 200 octopus cells are contacted by 12,000 fibres (Golding *et al.* 1995). The convergence of numerous sharply tuned inputs gives octopus cells broad tuning (Rhode *et al.* 1983). That octopus cells respond to coincident firing of auditory nerve inputs raises the question how these neurons deal with differences in timing produced by travelling wave delays (Fig. 1*B*). Inhibition has not been detected in octopus cells.

MSO neurons are bipolar, with ipsilateral and contralateral excitatory inputs segregated to the distal ends of lateral or medial dendritic arbors, respectively. MSO cells receive minimally two to four similarly and sharply tuned, excitatory axons per side (Couchman *et al.* 2010) (Fig. 1*B*). On each side MSO neurons form a sheet that holds a map of frequency in the dorsoventral dimension, but it is not yet clear whether there is a systematic mapping of best ITDs within the nucleus in all mammals (but see Yin & Chan, 1990, their Fig. 13). The dendrites of MSO neurons are thick and range between about 100 and 200 μm long but have relatively few branches (Smith, 1995; Rautenberg *et al.* 2009).

Glycinergic inhibition from both the medial and lateral nuclei of the trapezoid body is confined to the soma and proximal dendrites. The sensitivity to small differences in timing is aided by averaging of excitatory inputs and by inhibition (Brand *et al.* 2002; Chirila *et al.* 2007; Pecka *et al.* 2008).

The morphology of dendrites enhances coincidence detection in biologically relevant ways in both octopus and MSO cells. In octopus cells, electrotonic filtering by dendrites compensates for the travelling wave delays to produce large, rapidly rising summed EPSPs at the soma (McGinley *et al.* 2012). In MSO neurons, summation of subthreshold inputs is more effective and linear if they are distributed on both tufts than if they arise on a single tuft (Agmon-Snir *et al.* 1998). The large calibre of both octopus and MSO dendrites lowers axial resistance, speeding the flow of current from synapses to the soma and axon, thereby decreasing EPSP duration.

Synaptic transmission is specialized for temporal precision and reliability

mEPSCs are large and fast in octopus and MSO cells (750–900 pS, decay time constants 215–325 μs at 33–36°C)(Gardner *et al.* 1999; Cao *et al.* 2008). AMPA receptors include the rapidly gating flop variants of GluA4

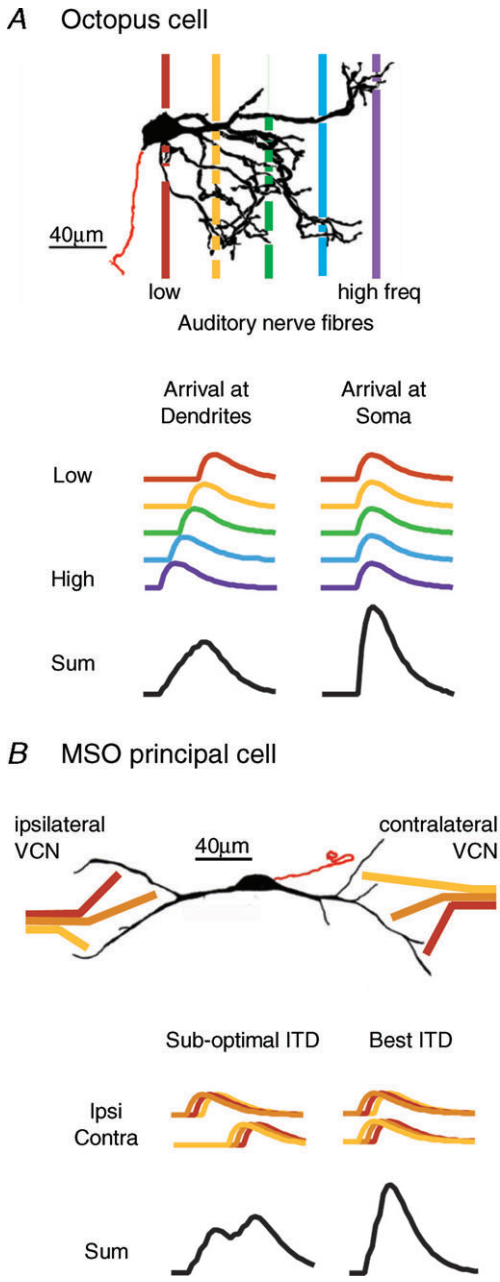

Figure 1. Octopus and MSO cells both detect coincidence in excitatory input
A, top panel, dendrites of octopus cells emanate from the rostral side of the cell body and spread across the tonotopic array of auditory nerve fibres where they are closely bundled as they pass from the ventral to the dorsal cochlear nucleus. The beginning of the axon is shown in red. Thus, cell bodies receive input from fibres tuned to the lowest frequencies (red) and the tips of dendrites receive inputs from fibres tuned to the highest frequencies (purple). (Cell is reproduced with permission from Golding *et al.* 1995.) Bottom panel, octopus cells detect coincident firing in groups of auditory nerve fibres (>60 in mice). Dendritic filtering makes octopus cells most sensitive to soma-directed sweeps of excitation that match the sweep of excitation produced by the cochlear travelling wave. *B*, top panel, MSO cells detect coincident firing of 2 to 5 ipsi- and 2 to 5 contralateral excitatory inputs tuned to similar low frequencies. The principal cells of the MSO are bipolar, with sparsely branching lateral and medial dendrites receiving inputs from ipsi- and contralateral sides, respectively. Tuning of MSO neurons is biased toward low frequencies. Bottom panel, the timing of MSO inputs at the soma reflects random differences in dendritic location. MSO neurons detect the coincidence in the average summed excitatory inputs from each side.

subunits, perhaps with GluA3 (Caicedo & Eybalin, 1999; Gardner *et al.* 1999, 2001; Schmid *et al.* 2001; Yang *et al.* 2011). EPSCs evoked in octopus cells by stimulating the fibre bundle rise over ∼0.5 ms and fall with decay time constants ∼0.7 ms (Cao & Oertel, 2010). Octopus and MSO cells preserve the timing of fast synaptic currents as rapidly rising and falling EPSPs. Depression is evident when synapses are stimulated repetitively (Cao *et al.* 2008; Cao & Oertel, 2010; Couchman *et al.* 2010). In responses to a train of clicks at 500 Hz to which an octopus cell fires in response to every click, a 200 μs shift in latency is evident over the first 10 clicks that probably reflects synaptic depression *in vivo* (Oertel *et al.* 2000). NMDA receptors are present at these synapses in mature animals, but their functional impact decreases with age, in part because g_{KL} activation by the AMPA component of EPSPs accelerates membrane repolarization and masks NMDA receptor-mediated depolarization (Cao & Oertel, 2010; Couchman *et al.* 2012).

Inhibition differs between octopus and MSO neurons. In octopus cells of mice glycinergic and GABAergic inhibition is physiologically undetectable whereas in MSO cells precisely timed glycinergic currents arising from two to four strong inputs influence both the location and magnitude of ITD curves (Brand *et al.* 2002; Magnusson *et al.* 2005; Couchman *et al.* 2010).

Low-voltage-activated K^+ (g_{KL}) and hyperpolarization-activated (g_h) conductances shape synaptic integration

Both octopus and MSO cells exhibit unusually low input resistances and transient firing in response to depolarizing current steps (Fig. 2*A* and *B*). Underlying these properties are two large, voltage-sensitive conductances that mediate opposing currents. A depolarization-activated, outward, low-voltage-activated K^+ current, I_{KL}, opposes a hyperpolarization-activated inward current, I_h (Oertel *et al.* 2000; Mathews *et al.* 2010; Cao & Oertel, 2011) (Fig. 2*C*). I_{KL} is mediated through ion channels of the KCNA family that reside in somatic and dendritic membranes of both octopus and MSO cells (Bal & Oertel, 2001; Scott *et al.* 2005; Oertel *et al.* 2008; Mathews *et al.* 2010). In MSO dendrites, measurements with outside-out patches showed that the density of g_{KL} is ∼3 times greater in the soma *versus* the dendrites and serves to sharpen

coincidence detection between the two dendritic tufts (Mathews *et al.* 2010). Activation and deactivation of g_h is slow relative to the duration of EPSPs while g_{KL} is activated by EPSPs and accelerates their repolarization (Golding *et al.* 1995; Scott *et al.* 2005). The activation of both conductances contributes to the low input resistance that confers short time constants, ~200 μs in octopus cells (Golding *et al.* 1999) and ~250 μs in mature MSO neurons (Scott *et al.* 2005; Couchman *et al.* 2010) (Fig. 2*A* and *B*). It also affects spatial summation of EPSPs in dendrites (Mathews *et al.* 2010; McGinley *et al.* 2012). The presence of any conductance in dendrites increases the attenuation of EPSPs and action potentials; the influence of g_{KL} on the spread of EPSPs along dendrites thus dynamically changes during the course of EPSP trains.

Hyperpolarization and cyclic nucleotide-gated (HCN) channels mediate an inward, non-inactivating current, I_h, that is partially activated at rest (Bal & Oertel, 2000; Oertel *et al.* 2008; Khurana *et al.* 2011, 2012) (Fig. 2*C*). The underlying conductance, g_h, reduces the membrane time constant by ~500%. This large change reflects the high density of g_h, as well as intracellular modulators such as cyclic AMP, which depolarize the activation range of the channel so that 41–48% of g_h is activated at rest. g_h also acts indirectly by depolarizing the resting potential of octopus and MSO cells (by 10 and 13 mV, respectively) and recruiting g_{KL} (Golding *et al.* 1999; Bal & Oertel, 2001; Khurana *et al.* 2011).

At rest I_{KL} and I_h are equal in magnitude and opposite in direction in octopus cells. The finding that the expression of g_h and g_{KL} co-varies between mouse strains suggests that g_{KL} and g_h are co-regulated (Oertel *et al.* 2000; Cao & Oertel, 2011).

Speed and security of action potential generation

The firing of action potentials represents the final outcome of dendritic coincidence detection. Octopus cells detect synchronous activation of subthreshold EPSPs from populations of auditory nerve fibres tuned to a range of frequencies. MSO cells also assess synchrony of

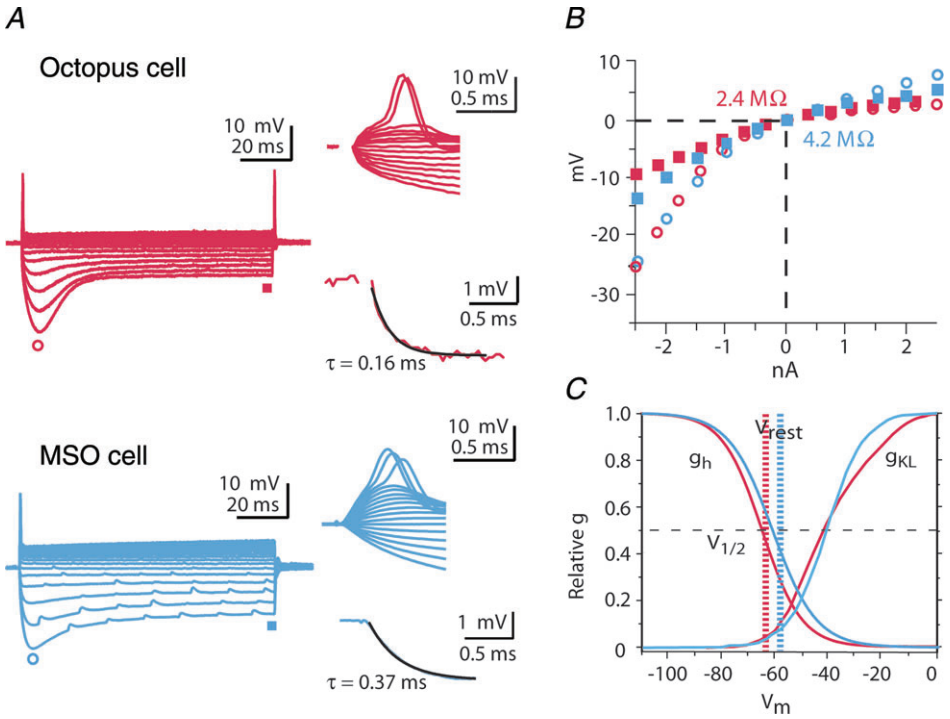

Figure 2. Responses to current reflect the presence of two voltage-sensitive conductances, g_h and g_{KL}
A, whole-cell recordings from an octopus and an MSO cell show the influence of g_h and g_{KL}. Responses are to a family of current pulses (−2.5 to +2.5 nA in 0.4 or 0.5 nA increments). Large depolarizing currents evoke a single action potential followed by a small steady depolarization, reflecting the shunting and hyperpolarizing influence of g_{KL}. Action potentials recorded at the cell body are small. Hyperpolarizing current pulses evoke a large hyperpolarization that sags toward rest, reflecting the slowly developing depolarization by g_h. Octopus cells often fire at the offset of hyperpolarizing pulses. Single exponentials fit to voltage changes within 3 mV of rest have time constants <0.5 ms. (Traces from octopus cells are adapted from Fig. 2 of Golding *et al.* 1999, with permission.) *B*, the voltage–current relations of the octopus and MSO cells in *A* from rest are similar. Input resistances near rest are <5 MΩ. *C*, summary of measurements of the voltage sensitivity of g_h and g_{KL} in octopus (red) and MSO (blue) cells measured under similar conditions (Bal & Oertel, 2000; Bal & Oertel, 2001; Mathews *et al.* 2010; Khurana *et al.* 2012). At the resting potential, opposing currents with opposite voltage sensitivity are partially activated.

subthreshold inputs to fire but synchrony is determined by whether the ITD is offset by an internal delay such as a difference in conduction velocity or path length that is introduced by the neuronal circuitry (Joris & Yin, 2007).

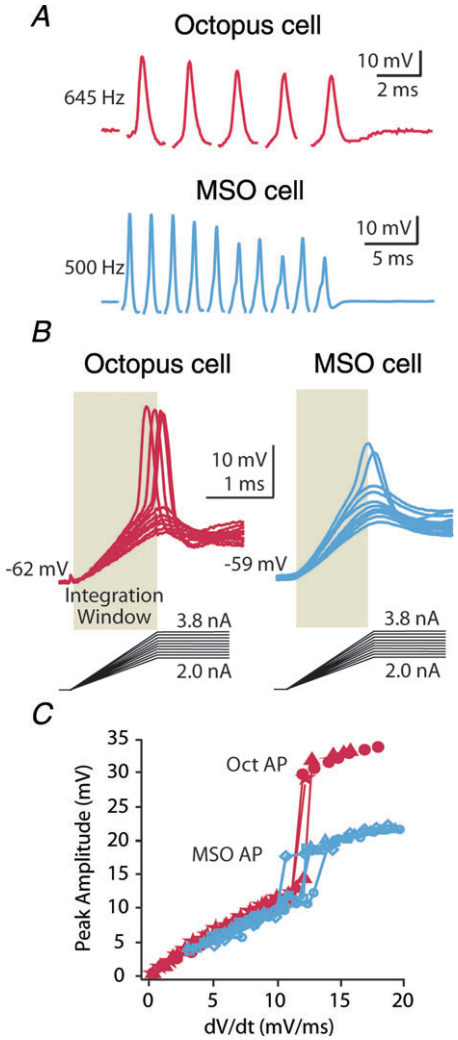

Figure 3. Octopus and MSO cells require rapid depolarization to fire
A, octopus and MSO cells are capable of responding to suprathreshold EPSPs at frequencies of >500 Hz. (Trace from octopus cell is adapted from Fig. 8 of Golding *et al.* 1995, with permission.) *B*, the activation of g_{KL} by 1.2 ms ramps of current prevents firing when depolarization is too slow, conferring a dependence of firing on a threshold rate of depolarization. Octopus and MSO cells integrate depolarization over a time window of about 1 ms (shaded areas). (Data on octopus cells are adapted from Fig. 3 of Ferragamo & Oertel, 2002; Michael T. Roberts provided the unpublished recording from the MSO cell.) *C*, plot of the amplitude of the response to current ramps shown in *B* shows a jump when they reach threshold (Δ). Plot also shows responses to 1.0 ms (O) and 1.4 ms (□) ramps to the same current levels. The octopus and MSO cells in *B* have rate of depolarization thresholds between 10 and 13 mV ms^{-1}. (Data in *C* from octopus cell is from Fig. 3 of Ferragamo & Oertel, 2002, with permission. MSO data are from the same cell as in *B*.)

Action potentials in octopus and MSO cells are precisely timed and can fire reliably even at high frequencies. *In vitro,* both can be driven up to 1000 spikes s^{-1} synaptically or with injected current (Oertel *et al.* 2000; Scott *et al.* 2007) (Fig. 3*A*). *In vivo,* octopus cells fire cycle for cycle in response to loud tones of up to 800 Hz (Rhode & Smith, 1986); they respond to every click in a train at 500 Hz with temporal jitter <200 μs (Oertel *et al.* 2000). MSO neurons' average firing rates are more limited *in vivo*, being generally less than 300 Hz. This is probably related to the short-term dynamics of excitatory synapses and possibly to the presence of inhibition in the MSO (Pecka *et al.* 2008). However, like octopus cells, MSO neurons fire precisely in response to acoustic stimuli (Goldberg & Brown, 1969), and exhibit better phase locking to tones than the auditory nerve (Yin & Chan, 1990).

Among the striking aspects of the physiology of octopus and MSO cells is the small and variable size of their action potentials, which range from 5 to 25 mV in the soma (Golding *et al.* 1999; Scott *et al.* 2005, 2007) (Figs 2*A*, and 3*A* and *B*). Action potentials are all or none, tetrodotoxin sensitive and easily recorded from axons (Smith *et al.* 2005). They are larger at lower temperatures when g_{KL} is reduced *in vitro* (Cao & Oertel, 2005) and they shrink from about 60 mV to 10 mV as animals mature (Scott *et al.* 2005). Direct measurements in MSO neurons show that action potentials are generated in the axon and decrement steeply as they propagate back to the soma and dendrites (Scott *et al.* 2007). g_{KL} contributes to their repolarization and actively suppresses their invasion of the dendrites (Golding *et al.* 1999; Ferragamo & Oertel, 2002; Svirskis *et al.* 2002; Scott *et al.* 2007). While voltage-gated sodium channels are expressed at the soma of MSO neurons, ~95% of these channels are inactivated at the resting potential (Scott *et al.* 2007). It is likely that attenuation of spikes from the axon to the soma and dendrites is dictated extensively by passive cable properties, an unfavourable ratio of sodium to potassium currents at the soma and perhaps in the initial segment itself. These factors electrically isolate the spike generation in the axon from the soma and dendrites, where summation of synaptic inputs takes place. The need for such electrical isolation becomes apparent considering the fact that the afterhyperpolarization of a conventionally sized spike would distort the amplitude and timing of future cycles of synaptic coincidence detection at the high frequencies exhibited by synaptic inputs. Isolation is necessarily incomplete because EPSPs from the soma must be able to drive action potentials.

Thresholds of action potentials are sensitive to the rate of depolarization of EPSPs. Slow depolarization raises thresholds by activating g_{KL} and inactivating Na^+ channels. Octopus and MSO cells thus act as differentiators, integrating depolarization over only about 1 ms and requiring depolarization to exceed

about 10 mV ms^{-1} (Ferragamo & Oertel, 2002; Svirskis *et al.* 2004; McGinley & Oertel, 2006) (Fig. 3*B* and *C*). Sensitivity to the rate of depolarization sharpens coincidence detection; the more asynchronous the inputs, the slower the rise of the resultant summed EPSP and the less likely it will be to elicit an action potential.

Concluding remarks

The computations that neurons perform depend on the time course over which they take place. If the integration time is long relative to the firing rate, neurons serve as 'integrators' and if they are short relative to the firing rate of inputs, neurons serve as 'coincidence detectors' (Konig *et al.* 1996). Octopus and MSO cells are arguably the most sensitive coincidence detectors in the brain, as they make use of acoustic information that is contained in differences in timing of tens to hundreds of microseconds, time periods that in most neurons are within the temporal jitter in firing. The morphological and biophysical properties of their dendrites enhance coincidence detection. Octopus cells use dendrites to compensate for the cochlear travelling wave delay of their inputs. MSO cells use dendrites to sharpen coincidence detection of inputs from two sides. Both neurons isolate the somatodendritic from the axonal compartments to an unusual extent. The precision required for proper functioning of these neurons raises the question how their morphological and biophysical properties develop and are regulated.

References

Adams JC (1997). Projections from octopus cells of the posteroventral cochlear nucleus to the ventral nucleus of the lateral lemniscus in cat and human. *Auditory Neurosci* **3**, 335–350.

Agmon-Snir H, Carr CE & Rinzel J (1998). The role of dendrites in auditory coincidence detection. *Nature* **393**, 268–272.

Bal R & Oertel D (2000). Hyperpolarization-activated, mixed-cation current (Ih) in octopus cells of the mammalian cochlear nucleus. *J Neurophysiol* **84**, 806–817.

Bal R & Oertel D (2001). Potassium currents in octopus cells of the mammalian cochlear nuclei. *J Neurophysiol* **86**, 2299–2311.

Brand A, Behrend O, Marquardt T, McAlpine D & Grothe B (2002). Precise inhibition is essential for microsecond interaural time difference coding. *Nature* **417**, 543–547.

Burger RM, Fukui I, Ohmori H & Rubel EW (2011). Inhibition in the balance: binaurally coupled inhibitory feedback in sound localization circuitry. *J Neurophysiol* **106**, 4–14.

Caicedo A & Eybalin M (1999). Glutamate receptor phenotypes in the auditory brainstem and mid-brain of the developing rat. *Eur J Neurosci* **11**, 51–74.

Cao XJ, McGinley MJ & Oertel D (2008). Connections and synaptic function in the posteroventral cochlear nucleus of deaf jerker mice. *J Comp Neurol* **510**, 297–308.

Cao X & Oertel D (2005). Temperature affects voltage-sensitive conductances differentially in octopus cells of the mammalian cochlear nucleus. *J Neurophysiol* **94**, 821–832.

Cao XJ & Oertel D (2010). Auditory nerve fibers excite targets through synapses that vary in convergence, strength, and short-term plasticity. *J Neurophysiol* **104**, 2308–2320.

Cao XJ & Oertel D (2011). The magnitudes of hyperpolarization-activated and low-voltage-activated potassium currents co-vary in neurons of the ventral cochlear nucleus. *J Neurophysiol* **106**, 630–640.

Carr CE & Konishi M (1990). A circuit for detection of interaural time differences in the brain stem of the barn owl. *J Neurosci* **10**, 3227–3246.

Chirila FV, Rowland KC, Thompson JM & Spirou GA (2007). Development of gerbil medial superior olive: integration of temporally delayed excitation and inhibition at physiological temperature. *J Physiol* **584**, 167–190.

Couchman K, Grothe B & Felmy F (2010). Medial superior olivary neurons receive surprisingly few excitatory and inhibitory inputs with balanced strength and short-term dynamics. *J Neurosci* **30**, 17111–17121.

Couchman K, Grothe B & Felmy F (2012). Functional localization of neurotransmitter receptors and synaptic inputs to mature neurons of the medial superior olive. *J Neurophysiol* **107**, 1186–1198.

Ferragamo MJ & Oertel D (2002). Octopus cells of the mammalian ventral cochlear nucleus sense the rate of depolarization. *J Neurophysiol* **87**, 2262–2270.

Gardner SM, Trussell LO & Oertel D (1999). Time course and permeation of synaptic AMPA receptors in cochlear nuclear neurons correlate with input. *J Neurosci* **19**, 8721–8729.

Gardner SM, Trussell LO & Oertel D (2001). Correlation of AMPA receptor subunit composition with synaptic input in the mammalian cochlear nuclei. *J Neurosci* **21**, 7428–7437.

Godfrey DA, Kiang NYS & Norris BE (1975). Single unit activity in the posteroventral cochlear nucleus of the cat. *J Comp Neurol* **162**, 247–268.

Goldberg JM & Brown PB (1969). Response of binaural neurons of dog superior olivary complex to dichotic tonal stimuli: some physiological mechanisms of sound localization. *J Neurophysiol* **32**, 613–636.

Golding NL, Ferragamo MJ & Oertel D (1999). Role of intrinsic conductances underlying responses to transients in octopus cells of the cochlear nucleus. *J Neurosci* **19**, 2897–2905.

Golding NL, Robertson D & Oertel D (1995). Recordings from slices indicate that octopus cells of the cochlear nucleus detect coincident firing of auditory nerve fibers with temporal precision. *J Neurosci* **15**, 3138–3153.

Henkel CK (1997). Axonal morphology in fibrodendritic laminae of the dorsal nucleus of the lateral lemniscus: afferent projections from the medial superior olivary nucleus. *J Comp Neurol* **380**, 136–144.

Henkel CK & Spangler KM (1983). Organization of the efferent projections of the medial superior olivary nucleus in the cat as revealed by HRP and autoradiographic tracing methods. *J Comp Neurol* **221**, 416–428.

Jeffress LA (1948). A place theory of sound localization. *J Comp Physiol Psychol* **41**, 35–39.
Joris P & Yin TC (2007). A matter of time: internal delays in binaural processing. *Trends Neurosci* **30**, 70–78.
Khurana S, Liu Z, Lewis AS, Rosa K, Chetkovich D & Golding NL (2012). An essential role for modulation of hyperpolarization-activated current in the development of binaural temporal precision. *J Neurosci* **32**, 2814–2823.
Khurana S, Remme MW, Rinzel J & Golding NL (2011). Dynamic interaction of Ih and IK-LVA during trains of synaptic potentials in principal neurons of the medial superior olive. *J Neurosci* **31**, 8936–8947.
Konig P, Engel AK & Singer W (1996). Integrator or coincidence detector? The role of the cortical neuron revisited. *Trends Neurosci* **19**, 130–137.
McGinley MJ, Liberman MC, Bal R & Oertel D (2012). Generating synchrony from the asynchronous: compensation for cochlear traveling wave delays by the dendrites of individual brainstem neurons. *J Neurosci* **32**,9301–9311.
McGinley MJ & Oertel D (2006). Rate thresholds determine the precision of temporal integration in principal cells of the ventral cochlear nucleus. *Hear Res* **216–217**, 52–63.
Magnusson AK, Kapfer C, Grothe B & Koch U (2005). Maturation of glycinergic inhibition in the gerbil medial superior olive after hearing onset. *J Physiol* **568**, 497–512.
Maier JK & Klump GM (2006). Resolution in azimuth sound localization in the Mongolian gerbil (*Meriones unguiculatus*). *J Acoust Soc Am* **119**, 1029–1036.
Mathews PJ, Jercog PE, Rinzel J, Scott LL & Golding NL (2010). Control of submillisecond synaptic timing in binaural coincidence detectors by K_v1 channels. *Nat Neurosci* **13**, 601–609.
Mills AW (1958). On the minimum audible angle. *J Acoust Soc Am* **30**, 237–246.
Nordeen KW, Killackey HP & Kitzes LM (1983). Ascending auditory projections to the inferior colliculus in the adult gerbil, *Meriones unguiculatus*. *J Comp Neurol* **214**, 131–143.
Oertel D, Bal R, Gardner SM, Smith PH & Joris PX (2000). Detection of synchrony in the activity of auditory nerve fibers by octopus cells of the mammalian cochlear nucleus. *Proc Nat Acad Sci U S A* **97**, 11773–11779.
Oertel D, Shatadal S & Cao XJ (2008). In the ventral cochlear nucleus Kv1.1 and subunits of HCN1 are colocalized at surfaces of neurons that have low-voltage-activated and hyperpolarization-activated conductances. *Neuroscience* **154**, 77–86.
Pecka M, Brand A, Behrend O & Grothe B (2008). Interaural time difference processing in the mammalian medial superior olive: the role of glycinergic inhibition. *J Neurosci* **28**, 6914–6925.
Rautenberg PL, Grothe B & Felmy F (2009). Quantification of the three-dimentional morphology of coincidence detector neurons in the medial superior olive of gerbils during late postnatal development. *J Comp Neurol* **517**, 385–396.
Rhode WS, Oertel D & Smith PH (1983). Physiological response properties of cells labeled intracellularly with horseradish peroxidase in cat ventral cochlear nucleus. *J Comp Neurol* **213**, 448–463.
Rhode WS & Smith PH (1986). Encoding timing and intensity in the ventral cochlear nucleus of the cat. *J Neurophysiol* **56**, 261–286.
Ruggero MA (1992). Physiology and coding of sound in the auditory nerve. In *The Mammalian Auditory Pathway: Neurophysiology*, eds. Popper AN & Fay RR, pp. 34–93. Springer-Verlag, New York.
Schmid S, Guthmann A, Ruppersberg JP & Herbert H (2001). Expression of AMPA receptor subunit flip/flop splice variants in the rat auditory brainstem and inferior colliculus. *J Comp Neurol* **430**, 160–171.
Schofield BR (1995). Projections from the cochlear nucleus to the superior paraolivary nucleus in guinea pigs. *J Comp Neurol* **360**, 135–149.
Scott LL, Hage TA & Golding NL (2007). Weak action potential backpropagation is associated with high-frequency axonal firing capability in principal neurons of the gerbil medial superior olive. *J Physiol* **583**, 647–661.
Scott LL, Mathews PJ & Golding NL (2005). Posthearing developmental refinement of temporal processing in principal neurons of the medial superior olive. *J Neurosci* **25**, 7887–7895.
Smith PH (1995). Structural and functional differences distinguish principal from nonprincipal cells in the guinea pig MSO slice. *J Neurophysiol* **73**, 1653–1667.
Smith PH, Massie A & Joris PX (2005). Acoustic stria: anatomy of physiologically characterized cells and their axonal projection patterns. *J Comp Neurol* **482**, 349–371.
Svirskis G, Kotak V, Sanes DH & Rinzel J (2002). Enhancement of signal-to-noise ratio and phase locking for small inputs by a low-threshold outward current in auditory neurons. *J Neurosci* **22**, 11019–11025.
Svirskis G, Kotak V, Sanes DH & Rinzel J (2004). Sodium along with low-threshold potassium currents enhance coincidence detection of subthreshold noisy signals in MSO neurons. *J Neurophysiol* **91**, 2465–2473.
Yang YM, Aitoubah J, Lauer AM, Nuriya M, Takamiya K, Jia Z, May BJ, Huganir RL & Wang LY (2011). GluA4 is indispensable for driving fast neurotransmission across a high-fidelity central synapse. *J Physiol* **589**, 4209–4227.
Yin TC & Chan JC (1990). Interaural time sensitivity in medial superior olive of cat. *J Neurophysiol* **64**, 465–488.

Acknowledgements

We are grateful to Michael Roberts for supplying the recording in Fig. 3 and for his excellent editorial suggestions. We also thank Xiao-Jie Cao, Samantha Wright and Arthur Sugden for their thoughtful comments on the manuscript. This work is supported by grants from NIH DC00176 to D.O. and NIH DC006788 to N.L.G.